ARTICLES

Photophysics and Photochemistry of Planar Alkylanthraquinones (the 1-Methyl and 1,4-Dimethyl Compounds) Studied by Subpicosecond and Nanosecond Laser Photolysis as Well as Steady-State Photolysis

Toshihiro Nakayama, Yukiyoshi Torii, Tetsuhiko Nagahara, Sadao Miki, and Kumao Hamanoue*

Department of Chemistry, Kyoto Institute of Technology, Matsugasaki, Sakyo-ku, Kyoto 606-8585, Japan

Received: August 13, 1998; In Final Form: October 27, 1998

By means of subpicosecond and nanosecond laser photolysis of the title compounds (MAQ and DMAQ), it is concluded that both the lowest excited singlet and triplet states undergo intramolecular hydrogen-atom transfer and the corresponding excited biradicals thus generated yield 9-hydroxy-1,10-anthraquinone-1-methide from MAQ and 9-hydroxy-4-methyl-1,10-anthraquinone-1-methide from DMAQ. Although these methides are stable at 77 K, they revert to the original anthraquinones at a higher temperature than 77 K. In ethanol and EPA (diethyl ether−isopentane−ethanol in 5:5:2 volume ratio) at room temperature, furthermore, 313 or 366 nm steady-state photolysis reveals that 1-methyl-9,10-dihydroxyanthracene ($MAQH_2$) is formed from MAQ irrespective of the excitation wavelength but 1,4-dimethyl-9,10-dihydroxyanthracene ($DMAQH_2$) is formed from DMAQ only upon 313 nm excitation. Undoubtedly, the lowest excited triplet state of MAQ abstracts a hydrogen atom from ethanol generating the semiquinone radical followed by formation of $MAQH_2$. In contrast, not the lowest excited triplet state but the third excited singlet or triplet state of DMAQ may abstract a hydrogen atom from ethanol yielding $DMAQH_2$ finally.

Introduction

In connection with the interest in the excited-state behavior of aromatic carbonyl compounds, we studied the photophysics and photochemistry of several sterically strained anthraquinones. Our findings were as follows: (1) The lowest excited triplet states of α-haloanthraquinones (the bromo and chloro compounds)[1] and *tert*-butylanthraquinones (the 1,2-di-*tert*-butyl-3-trimethylsilyl and 1,2,3-tri-*tert*-butyl compounds)[2] were unusually short-lived but their phosphorescence spectra were very broad with spectral profiles similar to those of the usual mixed $n\pi^*-\pi\pi^*$- or $\pi\pi^*$-type phosphorescence spectra. (2) 313 nm steady-state photolysis of α-haloanthraquinones in ethanol at room temperature yielded α-halo-9,10-dihydroxyanthracenes but the rate of photoreduction decreased with increasing triplet $\pi\pi^*$ character.[3] Formation of these reduced compounds upon 366 nm steady-state photolysis, however, was followed by photochemical dehydrohalogenation yielding α-haloanthraquinones (or anthraquinone) with one less halogen atom than the original anthraquinones and thus the final product was 9,10-dihydroxyanthracene, whereas no such photochemical dehydrohalogenation was observed for β-halo-9,10-dihydroxyanthracenes. (3) Formation of a hemi-Dewar-type isomer upon photolysis of 1,2-di-*tert*-butyl-3-trimethylsilylanthraquinone or 1,2,3-tri-*tert*-butylanthraquinone reported by Miki et al.[4] could be ascribed to valence isomerization in the lowest excited singlet state.[5] (4) The decay channels for the lowest excited singlet state of naphthoylnaphthvalene (NNV) were found to be intersystem crossing to the lowest excited triplet state (^{3}NNV*) and valence isomerization yielding ground-state naphthoylnaphthalene (NN) via an intermediate (probably a zwitterionic species).[6] Although ^{3}NNV* populated in ethanol abstracted a hydrogen atom from the solvent molecule generating the NNV ketyl radical, this radical also underwent rapid valence isomerization and recombination of two NN ketyl radicals thus formed yielded 1,1,2,2-tetra-(2-naphthyl)-1,2-ethanediol (naphthopinacol).

For 1,4-hexyl-bridged anthraquinone (HBAQ) with a benzene ring deformed to a boat form, we also studied photoinduced intramolecular hydrogen-atom transfer from the benzylic methylene to the carbonyl oxygen and the following results were obtained;[7] (i) the reaction was originated from both the lowest excited singlet and triplet states forming the ground-state singlet biradical and its methide (1,4-hexylidene-bridged 9-hydroxyanthracene-10-one) in equilibrium; (ii) although these products were stable in EPA (diethyl ether−isopentane−ethanol in 5:5:2 volume ratio) at 77−140 K, they (or one of them) produced at room temperature changed to 1,4-hexylidene-bridged anthraquinone (product **1**) in aprotic solvents such as benzene, toluene, methylcyclohexane and 2-methyltetrahydrofuran, or to product **1** (minor) and 1,4-hexyl-bridged 1,4-diethoxy-9,10-dihydroxyanthracene (product **2**, major) in ethanol and EPA; (iii) interconversion of products **1** ⇌ **2** by the change of an aprotic solvent ⇌ ethanol (or EPA) and slow thermal reversion of products **1** and **2** to the original anthraquinone (HBAQ) could also be seen at room temperature.

As an extension of our studies on the photophysics and photochemistry of substituted anthraquinones, the present paper

* Corresponding author.

10.1021/jp9833653 CCC: $18.00 © 1999 American Chemical Society
Published on Web 03/05/1999

deals with the photochemical behavior of planar alkylanthraquinones such as 1-methylanthraquinone (MAQ) and 1,4-dimethylanthraquinone (DMAQ). The subjects for the present study are (a) intramolecular hydrogen-atom transfer from the methyl group to the carbonyl oxygen in both the lowest excited singlet and triplet states of MAQ and DMAQ, and (b) intermolecular hydrogen-atom abstraction of the carbonyl oxygen from ethanol in the lowest excited triplet state of MAQ and the third excited singlet or triplet state of DMAQ. Although DMAQ seems to be a model compound for interpretation of the photochemistry of HBAQ, the excited-state behavior of MAQ is expected to be similar to not only that of anthraquinone but also those of DMAQ and HBAQ. Preliminary results have already been published elsewhere,[8] but the present study indicates that the previous interpretation of two decay rate constants (k'_{D_3} and k'_{D_4}) obtained in EPA at 77 K is incorrect.

Experimental Section

By a modification of the method for preparation of anthraquinone,[9] MAQ was synthesized by cyclization of 2-(2-methylbenzoyl)benzoic acid prepared by the Grignard reaction of phthalic anhydride with 2-tolylmagnesium bromide, and DMAQ was synthesized by cyclization of 2-(2,5-dimethylbenzoyl)benzoic acid prepared by the Friedel−Crafts reaction of phthalic anhydride with *p*-xylene; MAQ and DMAQ thus obtained were recrystallized from ethanol. The solvents used were benzene, hexane, ethanol, and EPA; although spectral-grade benzene (Dojin) and hexane (Dojin), and Uvasol diethyl ether (Merck) were used without further purification, spectral-grade ethanol (Nacalai) was dried using molecular sieves 3A (Wako) and GR-grade isopentane (Wako) was purified by passing it through an alumina column. The sample solutions used for subpicosecond laser photolysis in a flow cell of 2 mm path length were deoxygenated by bubbling of Ar gas, while those used for nanosecond laser photolysis and steady-state photolysis in a cell of 10 mm path length were degassed by several freeze−pump−thaw cycles; oxygen-saturated solutions used for nanosecond laser photolysis were prepared by bubbling of O_2 gas.

Subpicosecond laser photolysis was performed by a pump−probe method using a laser photolysis system comprising a femtosecond mode-locked Ti:sapphire oscillator (Tsunami, model 3960) and a regenerative amplifier (model TSA-50) from Spectra-Physics;[10] both intensities of the excitation light pulse (the 267 nm third harmonic) and the probing light pulse (the white-light continuum generated by focusing the 800 nm fundamental into water) were approximated by a Gaussian function with a full width at the half-maximum intensity (fwhm) of 0.25 ps. For nanosecond sample excitation, the second (347.2 nm, fwhm = 20 ns) or third (355 nm, fwhm = 5 ns) harmonic from a ruby or a Nd^{3+}:YAG laser, respectively, was used and the transient absorption spectra were recorded using a multichannel analyzer;[11] the intensity changes of transient absorptions with time were recorded by means of a combination of a photomultiplier (Hamamatsu R329 or R666) with an Iwatsu TS-8123 or a LeCroy 9360 storage oscilloscope. Steady-state photolysis was carried out using the 313 and 366 nm monochromatic lights selected from a USH-500D super-high-pressure mercury lamp, and the absorption spectral change upon photolysis was recorded using a Hitachi 200-20 spectrophotometer.

Results

Subpicosecond and Nanosecond Laser Photolysis of XAQ (MAQ or DMAQ) at Various Temperatures. Figure 1 shows the transient absorption spectra obtained by 267 nm subpicosecond laser photolysis of XAQ in ethanol at room temperature. Clearly, the decrease of band S at a shorter wavelength is accompanied with the increase of band B_1 at a longer wavelength and not only band B_1 but also bands $B_{2,3}$ for MAQ (or band B_3 for DMAQ) can be seen after the disappearance of band S; it is confirmed that the spectra obtained at 20 ps delay are identical to those obtained at 900 ps delay. As shown in Figure 2, furthermore, the transient absorption monitored at 380, 435, or 385 nm appears within the duration of subpicosecond pulse excitation and then decreases following a single-exponential function with a decay time (τ_D) equal to a rise time (τ_R) obtained for the single-exponential increase of a transient absorption monitored at 535 nm. This indicates that a transient species responsible for band S generates another transient species responsible for band B_1 and the lifetime of the former transient species is 2 ps for MAQ or 0.7 ps for DMAQ. Interestingly, Figure 1 indicates that band B_1 at a delay time shorter than 20 ps shifts with time to a longer wavelength and after then no such a shift can be seen. This progressive time-dependent shift

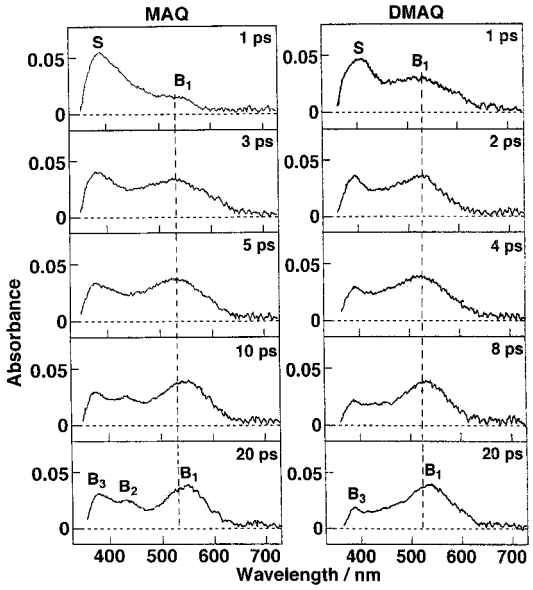

Figure 1. Transient absorption spectra obtained by 267 nm subpicosecond laser photolysis of MAQ and DMAQ in ethanol at room temperature.

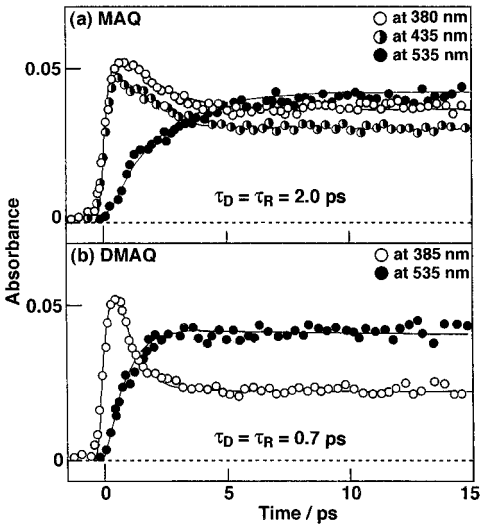

Figure 2. Time-dependent absorbance changes of transient absorptions obtained by 267 nm subpicosecond laser photolysis of MAQ and DMAQ in ethanol at room temperature.

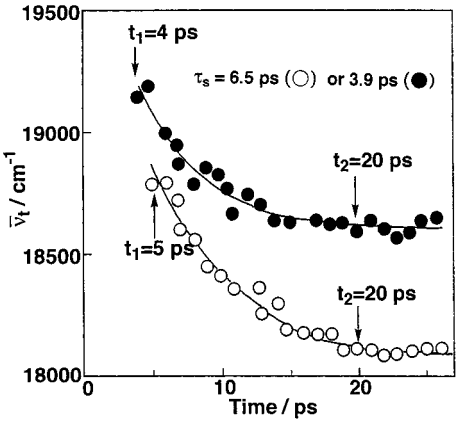

Figure 3. Plots of wavenumbers ($\bar{\nu}_t$) of the absorption maxima of band B_1 (○ for MAQ or ● for DMAQ) against the delay time (t). The solid curves are the best-fit single-exponential functions given by eq 1.

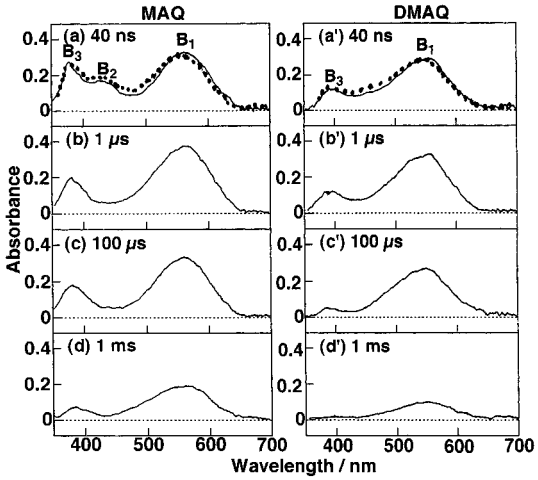

Figure 4. Transient absorption spectra (—) obtained by 347.2 nm nanosecond laser photolysis of MAQ and DMAQ in ethanol at room temperature. The dotted spectra are normalized ones obtained at 20 ps delay by subpicosecond pulse excitation.

of band B_1 up to 20 ps delay is very clearly seen in Figure 3, where the open (for MAQ) or closed (for DMAQ) circles are the wavenumbers ($\bar{\nu}_t$) of band maxima plotted against the delay time (t) and the solid curves are the best-fit functions given by eq 1; t_1 and t_2 (=20 ps) are delay times indicated in Figure 3, and τ_s is a time constant for the tentatively assumed single-exponential band shift.

$$\bar{\nu}_t = \bar{\nu}_{t_2} + (\bar{\nu}_{t_1} - \bar{\nu}_{t_2}) \exp[-(t - t_1)/\tau_s] \qquad (1)$$

In ethanol at room temperature, 347.2 nm nanosecond pulse excitation of XAQ using a ruby laser (fwhm = 20 ns) gives rise to the appearance of transient absorption spectra shown in Figure 4. Normalization of the spectra (the dotted lines) obtained

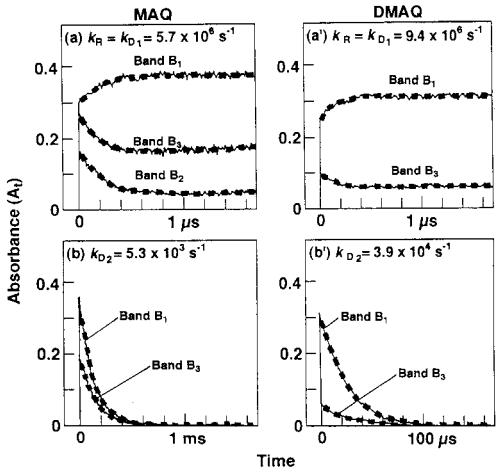

Figure 5. Changes in the absorbances (A_t) of bands B_1 (monitored at 540 nm for both MAQ and DMAQ), B_2 (monitored at 435 nm for MAQ), and B_3 (monitored at 380 nm for MAQ and 385 nm for DMAQ) with time obtained by 347.2 nm nanosecond laser photolysis of MAQ and DMAQ in ethanol at room temperature (solid curves). The dashed curves are best-fit single-exponential functions with rate constants ($k_R = k_{D_1}$, k_{D_2}) indicated.

at 20 ps delay by subpicosecond pulse excitation to those (the solid lines) obtained at the end of nanosecond pulse excitation (40 ns delay) reveals no spectral difference. As shown in Figure 5, furthermore, the absorbance (A_t at 540 nm) of band B_1 (appeared within the duration of nanosecond pulse excitation) further increases and then decreases to the zero absorbance following two single-exponential functions with rise and decay rate constants k_R and k_{D_2}, respectively. In contrast, A_t (at 380 nm for MAQ and 385 nm for DMAQ) of band B_3 (also appeared within the duration of nanosecond pulse excitation) decreases to the zero absorbance following two single-exponential functions with decay rate constants k_{D_1} and k_{D_2}. For MAQ, A_t (at 435 nm) of band B_2 decreases following a single-exponential function with decay rate constant k_{D_1} and Figure 4b reveals no existence of band B_2 at 1 μs delay. Since similar results are also obtained in EPA, benzene, hexane, and oxygen-saturated solvents (ethanol and benzene) at room temperature, all the rate constants obtained so far are listed in Table 1; even by 355 nm nanosecond pulse excitation using a Nd^{3+}:YAG laser (fwhm = 5 ns), however, the rate constants (k_R and k_{D_1}) in oxygen-saturated benzene are found to be greater than 10^8 s^{-1}.

The 347.2 nm nanosecond pulse excitation of XAQ in EPA at 77 K using a ruby laser (fwhm = 20 ns) gives rise to the appearance of transient absorption spectra shown in Figure 6. Although these spectra are similar to those obtained at room temperature (cf. Figure 4), both bands B_1 and B_3 observed at 77 K do not disappear completely even at a long delay time. As shown in Figure 7, furthermore, the absorbance changes of bands B_1, B_2, and B_3 with time observed at 77 K reveal the

TABLE 1: Rate Constants Obtained for the Rise (k_R) and Decay (k_{D_1}, k_{D_2}) of Transient Absorptions with Time Obtained in Ethanol, EPA, Benzene, and Hexane at Room Temperature

	MAQ		DMAQ	
solvent	$k_R = k_{D_1}$/s^{-1}	k_{D_2}/s^{-1}	$k_R = k_{D_1}$ /s^{-1}	k_{D_2} /s^{-1}
ethanol	$(5.7 \pm 0.2) \times 10^6$	$(5.3 \pm 0.2) \times 10^3$	$(9.4 \pm 0.1) \times 10^6$	$(3.9 \pm 0.2) \times 10^4$
+ O_2[a]	$(9.4 \pm 0.2) \times 10^6$	$(5.3 \pm 0.2) \times 10^3$	$(1.1 \pm 0.1) \times 10^7$	$(3.9 \pm 0.2) \times 10^4$
EPA	$(5.7 \pm 0.2) \times 10^6$	$(3.4 \pm 0.2) \times 10^4$	$(9.4 \pm 0.2) \times 10^6$	$(1.4 \pm 0.1) \times 10^5$
benzene	$(1.3 \pm 0.1) \times 10^7$	$(1.8 \pm 0.1) \times 10^6$	$(1.6 \pm 0.2) \times 10^7$	$(3.1 \pm 0.1) \times 10^6$
+ O_2[a]	$>10^8$	$(1.8 \pm 0.1) \times 10^6$	$>10^8$	$(3.1 \pm 0.1) \times 10^6$
hexane	$(1.5 \pm 0.2) \times 10^7$	$(3.1 \pm 0.2) \times 10^6$	$(1.8 \pm 0.2) \times 10^7$	$(3.3 \pm 0.2) \times 10^6$

[a] O_2 is saturated by its bubbling.

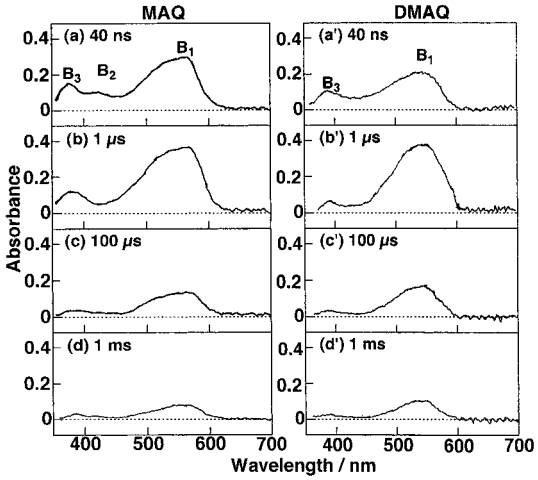

Figure 6. Transient absorption spectra obtained by 347.2 nm nanosecond laser photolysis of MAQ and DMAQ in EPA at 77 K.

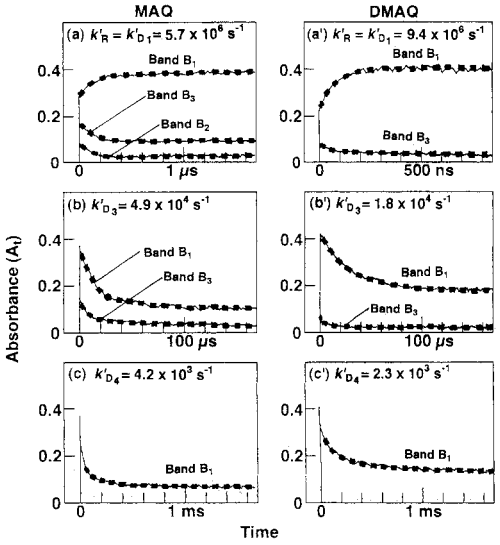

Figure 7. Changes in the absorbances (A_t) of bands B_1 (monitored at 540 nm for both MAQ and DMAQ), B_2 (monitored at 435 nm for MAQ), and B_3 (monitored at 380 nm for MAQ and 385 nm for DMAQ) with time obtained by 347.2 nm nanosecond laser photolysis of MAQ and DMAQ in EPA at 77 K (solid curves). The dashed curves are best-fit single-exponential functions with rate constants ($k'_R = k'_{D_1}$, k'_{D_3}, k'_{D_4}) indicated.

existence of three transient species (with rise and decay rate constants $k'_R = k'_{D_1}$, k'_{D_3}, and k'_{D_4})[12] and one nondecay component.

In comparison with the result obtained at room temperature (cf. Figure 5) with that obtained at 77 K (cf. Figure 7), it is expected that the changes of transient absorptions with time recorded at a higher temperature than 77 K should reveal the existence of four decay components owing to the disappearance of the residual absorption bands observed at 77 K. In order to confirm this, 347.2 nm nanosecond pulse excitation of XAQ in hexane at 177 K is performed using a ruby laser (fwhm = 20 ns) and Figure 8 really indicates the existence of four decay processes with rate constants [$k_R = k_{D_1} > k_{D_3}$ (corresponding to k'_{D_3}) > k_{D_4} (corresponding to k'_{D_4}) > k_{D_2}].[13]

Steady-State Photolysis of XAQ (MAQ or DMAQ) at 77 K and Room Temperature. As shown by the solid lines in Figure 9, 313 nm steady-state photolysis of XAQ in EPA at 77 K gives rise to the decrement of a reactant absorption band (R) accompanied with the appearance of three new absorption bands (P_1, P_2, and P_3). After photolysis, furthermore, elevation of the

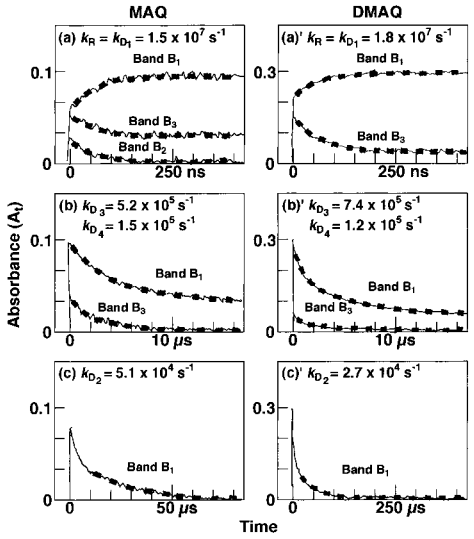

Figure 8. Changes in the absorbances (A_t) of bands B_1 (monitored at 540 nm for both MAQ and DMAQ), B_2 (monitored at 420 nm for MAQ), and B_3 (monitored at 380 nm for MAQ and 385 nm for DMAQ) with time obtained by 347.2 nm nanosecond laser photolysis of MAQ and DMAQ in hexane at 177 K (solid curves). The dashed curves are best-fit (a, c, a′, c′) single-exponential and (b, b′) biexponential functions with rate constants ($k_R = k_{D_1}$, k_{D_3}, k_{D_4}, k_{D_2}) indicated.

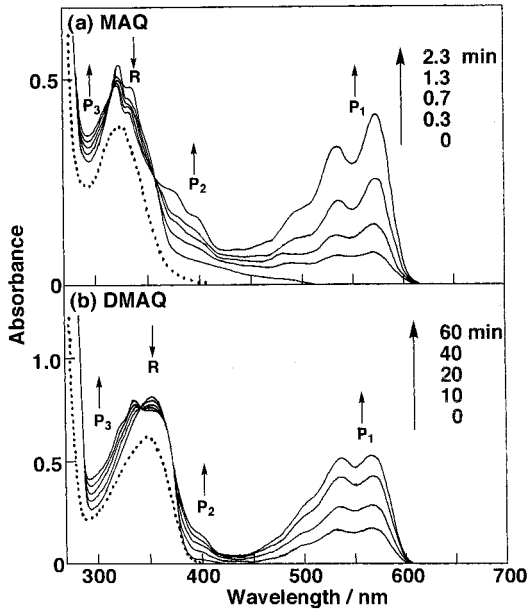

Figure 9. Absorption spectral change upon 313 nm steady-state photolysis of MAQ and DMAQ in EPA at 77 K (solid lines). The dotted spectra are recorded by elevation of the sample temperature up to room temperature after photolysis.

sample temperature up to room temperature causes the disappearance of bands P_{1-3} and only band R can be seen (cf. the dotted line). Similar results are also obtained by 366 nm steady-state photolysis of XAQ in EPA at 77 K. For the latter discussion, 530 nm nanosecond pulse excitation of the final product (responsible for bands P_{1-3} observed in EPA at 77 K) is performed using a Nd^{3+}:YAG laser (fwhm = 5 ns). Although no transient absorption can be seen, a short-lived fluorescence is detected. As shown in Figure 10, furthermore, the corresponding fluorescence spectrum (the dashed line) can be ascribed to the fluorescence originating from the lowest excited singlet state of the final product, because its absorption spectrum (the solid line) is almost identical to the fluorescence excitation spectrum (the dotted line).

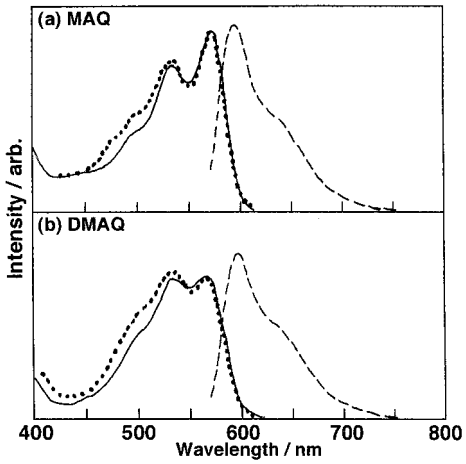

Figure 10. Fluorescence (– – –), its excitation (···) and absorption (—) spectra obtained for MT_b in EPA at 77 K.

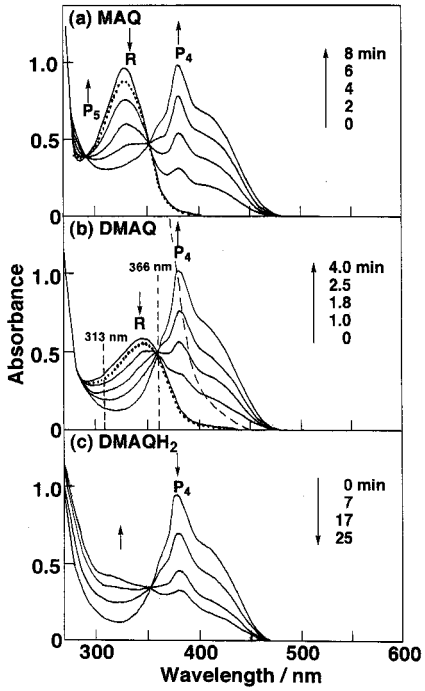

Figure 11. Absorption spectral change upon 313 nm steady-state photolysis of MAQ (a) and DMAQ (b) in ethanol at room temperature (solid lines); the dotted spectra are recorded by introducing air after photolysis. The absorption spectral change shown in (c) is obtained upon 366 nm steady-state photolysis of $DMAQH_2$ in ethanol at room temperature.

At room temperature, 313 or 366 nm steady-state photolysis of MAQ in benzene reveals no product formation but that in ethanol or EPA causes the absorption spectral change different from the result obtained in EPA at 77 K. A typical example obtained by 313 nm steady-state photolysis in ethanol at room temperature is shown in Figure 11a (the solid lines) and exposure of the sample solution to air after photolysis causes almost quantitative oxidation of the photoproduct back to the original anthraquinone (MAQ) as shown by the dotted spectrum.

For DMAQ in ethanol or EPA at room temperature, however, a photochemical reaction similar to that observed for MAQ is observed only upon 313 nm steady-state photolysis. A typical example obtained in ethanol is shown by the solid lines in Figure 11b, where the dotted spectrum also indicates almost quantitative oxidation of the photoproduct back to the original anthraquinone (DMAQ) upon introduction of air to the sample solution after photolysis. As shown in Figure 11c, furthermore, 366 nm steady-state photolysis of the photoproduct in ethanol at room temperature causes its spectral disappearance with no recovering to the original anthraquinone (DMAQ). Hence, no decrement in the reactant absorption upon 366 nm steady-state photolysis of DMAQ in ethanol and EPA at room temperature can not be ascribed to formation of the photoproduct followed by its subsequent photochemical conversion to the original anthraquinone (DMAQ).

SCHEME 1

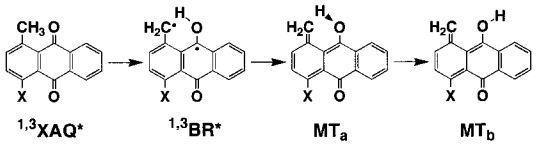

Discussion

Intramolecular Hydrogen-Atom Transfer from the Methyl Group to the Carbonyl Oxygen in Both the Lowest Excited Singlet and Triplet States of XAQ (MAQ or DMAQ). In EPA at 77 K, the residual absorption bands (responsible for the nondecay component) obtained by nanosecond laser photolysis (cf. Figures 6 and 7) are found to be identical to bands $P_{1,2}$ obtained by steady-state photolysis (cf. Figure 9). Similar absorption bands have also been observed for the several methides formed from 1,4-hexyl-bridged anthraquinone[7] and 1-alkylanthraquinones[14,15] as the stable products at 77 K. Since the absorptions of these methides also disappear upon elevation of the temperature up to room temperature, the photoproduct obtained for XAQ in EPA at 77 K can be identified to be the methide (MT_b), i.e., 9-hydroxy-1,10-anthraquinone-1-methide for MAQ or 9-hydroxy-4-methyl-1,10-anthraquinone-1-methide for DMAQ.

It is reported that the precursor of the enol formed from 5,8-dimethyl-1-tetralone is the excited triplet state of the enol form.[16−18] Upon nanosecond pulse excitation of MT_b in EPA at 77 K, however, no transient absorptions are detectable but the fluorescence (originating from the lowest excited singlet state of MT_b) can be seen as stated previously. By nanosecond laser photolysis of XAQ in EPA at 77 K, furthermore, no emissions are detectable during measurements of the transient absorption spectra shown in Figure 6. We thus believe that MT_b formed from XAQ is different from its ground-state singlet biradical and no excited singlet state of MT_b is formed upon photolysis of XAQ.

Two rotamers are reported for the enols of several aromatic ketones such as 2-methylacetophenone, 2-methylbenzophenone, 5,8-dimethyl-1-tetralone, 1,4-dimethylanthrone, and 3′,6′-dimethyldibenzosuberone.[19,20] As shown in Scheme 1, therefore, the existence of a rotamer (MT_a) of MT_b may also be expected and it is reasonable that MT_a is formed from both the excited singlet (^{1}BR*) and triplet (^{3}BR*) biradicals which are generated by intramolecular hydrogen-atom transfer from the methyl group to the carbonyl oxygen in the lowest excited singlet (^{1}XAQ*) and triplet (^{3}XAQ*) states of XAQ, respectively.

Al-Soufi et al.[18] reported the overlap of absorption spectra due to the excited triplet and ground states of the enol (formed from 5,8-dimethyl-1-tetralone), and Grellman et al.[19] reported the identical absorption spectra for the enol (Z-2 formed from 2-methylacetophenone) existing in two conformations. We thus believe that absorption bands of ^{1,3}BR* are similar to those of $MT_{a,b}$ and those of the latter two rotamers are indistinguishable in regard to the band profile and intensity. On the basis of these

SCHEME 2

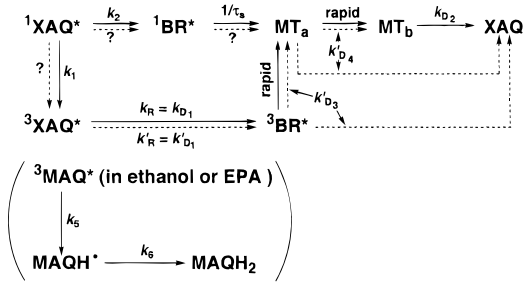

conjectures, the photochemistry of XAQ forming unstable MT_a and then MT_b at room temperature can be interpreted as in Scheme 2 (cf. the processes shown by the solid arrows in Scheme 2): (1) Band S appeared within the duration of subpicosecond pulse excitation is the singlet−singlet absorption of ^{1}XAQ* generating ^{1}BR* and the single-exponential shift of band B_1 with rate constant $1/\tau_s = 1.5 \times 10^{11}$ s^{-1} for MAQ (or $1/\tau_s = 2.6 \times 10^{11}$ s^{-1} for DMAQ) reflects formation of MT_a from ^{1}BR* followed by rapid conversion to MT_b. (2) Band B_2 (for MAQ) and the decay component in band B_3 (for both MAQ and DMAQ) with decay rate constant k_{D_1} observed by nanosecond laser photolysis are due to the triplet−triplet absorptions originating from ^{3}XAQ*, because the lowest excited triplet states of anthraquinone and haloanthraquinones have characteristic absorption bands (at ∼380−460 nm)[1,21] similar to bands B_2 and B_3. (3) A slow rise component in band B_1 with rate constant k_R ($=k_{D_1}$) thus reflects ^{3}XAQ* → ^{3}BR* hydrogen-atom transfer followed by rapid ^{3}BR* → MT_a → MT_b conversion, i.e., ^{3}BR* → MT_a process with spin conversion is also rapid. (4) The complete disappearance of bands B_1 and B_3 with decay rate constant k_{D_2} reflects MT_b → XAQ thermal reversion in accordance with no existence of MT_b upon steady-state photolysis of XAQ at room temperature. (5) The small rise and decay rate constants ($k_R = k_{D_1}$ and k_{D_2}) in ethanol and EPA compared with those in benzene and hexane (cf. Table 1) may reflect the greater stabilization of ^{3}XAQ* and MT_b in the former solvents than the latter solvents.

Since ^{1}XAQ* → ^{3}XAQ* intersystem crossing (with rate constant k_1) competes with ^{1}XAQ* → ^{1}BR* hydrogen-atom transfer (with rate constant k_2), the rate constant ($1/\tau_D = 1/\tau_R = 5.0 \times 10^{11}$ s^{-1} for MAQ or 1.4×10^{12} s^{-1} for DMAQ) obtained for the single-exponential decrease or increase of band S or B_1, respectively, should be equal to the sum of rate constants k_1 and k_2. If these two rate constants are comparable, therefore, the rate constant (∼10^{11} s^{-1}) estimated for ^{1}MAQ* → ^{1}BR* hydrogen-atom transfer by Gritsan et al.[15] may be correct. No ^{3}XAQ* → ^{3}BR* hydrogen-atom transfer can be seen by subpicosecond laser photolysis and the rate constants ($k_R = k_{D_1}$) listed in Table 1 are comparable with those reported for intramolecular hydrogen-atom transfer in the lowest excited triplet states of cyclic anthraquinones [1,4-hexyl-bridged anthraquinone ($(2.4-3.0) \times 10^6$ s^{-1})[7] and 5,8-dimethyl-1-tetralone (1.8×10^6 s^{-1})[18]] and acyclic *o*-alkylbenzophenoes [2,4-dimethylbenzophenone ($(2.6-3.6) \times 10^7$ s^{-1}) and 2-isopropylbenzophenone ($>5 \times 10^7$ s^{-1})].[22] We thus suspect the extremely large rate constant (2.9×10^{10} s^{-1} at 298 K) reported for ^{3}MAQ* → ^{3}BR* hydrogen-atom transfer by Gritsan et al.[15] Also this rate constant is 2 orders of magnitude greater than those obtained for the lowest excited triplet states of *o-tert*-butylbenzophenone ($>10^8$ s^{-1})[23] and 2-methylbenzophenone (4.0×10^8 s^{-1})[24] at room temperature. As discussed later, furthermore, no temperature effect on the rate constants ($k_R = k_{D_1}$) is observed. Hence, the temperature-dependent rate constants obtained by Gritsan et al.[15] are doubtful and conversion of the triplet $\sigma\pi$-biradical to the methide proposed by them can be ascribed to temperature-independent ^{3}MAQ* → ^{3}BR* hydrogen-atom transfer. Also, oxygen-assisted formation of the methide from the triplet $\sigma\pi$-biradical (probably ^{3}XAQ* as stated above) reported by Gritsan et al.[15] is doubtful, because $k_R = k_{D_1}$ obtained in the oxygen-saturated solvents are greater than those obtained in the deoxygenated solvents (cf. Table 1) but the increment of transient absorption reflecting formation of MT_a and then MT_b from ^{3}XAQ* is found to be suppressed.

All the rise and decay curves of transient absorptions as shown in Figure 5 can well be analyzed by the first-order reaction kinetics and the rate constants ($k_R = k_{D_1}$ and k_{D_2}) obtained in ethanol ([XAQ] = $(3-9) \times 10^{-4}$ M) and benzene ([XAQ] = $(0.4-2) \times 10^{-4}$ M) are found to be independent of the concentration ([XAQ]) of XAQ. Hence, a second-order reaction of two methides (probably MT_b) reverting to two MAQ observed in nonpolar solvents (hexane and toluene) at a lower temperature by Gritsan et al.[15] is doubtful. In fact, as shown in Figure 8, all the rise and decay curves of transient absorptions obtained by nanosecond laser photolysis of XAQ in hexane at 177 K can well be interpreted in terms of the first-order reaction kinetics; i.e., no intensity change of the transient absorption with time following the second-order reaction kinetics can be seen.

At 77 K, MT_b can exist as the stable product as stated previously. The rise and decay rate constants indicated in Figure 7 can be ascribed to those for the processes shown by the dashed arrows in Scheme 2, i.e., both the rapid ^{3}BR → MT_a and MT_a → MT_b processes at room temperature are suppressed at 77 K, and thus the interpretation in our previous papers[8] that k'_{D_3} and k'_{D_4} were the rate constants for the decay processes of ^{1}BR* and ^{3}BR*, respectively, is incorrect. Taking into account of the absorbances responsible for ^{3}BR*, MT_a, and MT_b shown in Figure 7, we believe that not only MT_a but also ^{3}BR* at 77 K undergoes reversion to the original compound (XAQ). For both MAQ and DMAQ in EPA, the rate constants ($k'_R = k'_{D_1}$) obtained at 77 K are equal to those ($k_R = k_{D_1}$) obtained at room temperature (cf. Figure 7 and Table 1). Also, $k_R = k_{D_1}$ obtained in hexane at 177 K (cf. Figure 8) are equal to those obtained at room temperature (cf. Table 1). Hence, intramolecular hydrogen-atom transfer originating from ^{3}XAQ* may be caused by tunneling of a hydrogen atom from the methyl group to the carbonyl oxygen. A similar temperature-independent intramolecular hydrogen-atom transfer is also observed for the lowest excited triplet state of 1,4-hexyl-bridged anthraquinone;[7] for the lowest excited triplet state of 5,8-dimethyl-1-tetralone, however, Al-Soufi et al.[18] reported temperature-dependent tunneling of a hydrogen atom from the methyl group to the carbonyl oxygen.

Intermolecular Hydrogen-Atom Abstraction of the Carbonyl Oxygen from Ethanol in the Lowest Excited Triplet State of MAQ. For photoreduction of anthraquinone and haloanthraquinones (the bromo and chloro compounds),[3,21] it is well-known that the carbonyl oxygen of the lowest excited triplet state abstracts a hydrogen atom from the solvent generating the semiquinone radical and then a disproportionation reaction of two semiquinone radicals yields 9,10-dihydroxyanthracenes and the original anthraquinones simultaneously. Bands P_4 and P_5 (especially band P_4) shown in Figure 11a are very similar to the absorption bands of 9,10-dihydroxyanthracenes stated above and these products also revert to the original anthraquinones upon introduction of air. Hence, the photoproduct responsible for bands $P_{4,5}$ can safely be identified to be 1-methyl-9,10-dihydroxyanthracene ($MAQH_2$) which is formed via the semiquinone radical ($MAQH^•$) generated by intermo-

lecular hydrogen-atom abstraction of ^{3}MAQ* from ethanol (cf. the processes shown in parentheses in Scheme 2).

In this case, the decay rate constant of ^{3}MAQ* (determined from the decay curve of band B_2 or B_3 shown in Figure 5a) should be equal to the sum of rate constants for generation of ^{3}BR* (with rate constant k_{D_1}) and MAQH$^\bullet$ (with rate constant k_5). Furthermore, the decay curve of band B_3 shown in Figure 5b should be analyzed by a combination of the first-order (with rate constant k_{D_2}) and the second-order (with rate constant k_6) reaction kinetics, because the semiquinone radicals of several anthraquinones also have absorption bands around 380 nm.[21] Despite these circumstances, all the decay curves of bands B_2 and B_3 as shown in Figure 5, a and b, can well be reproduced by a single-exponential function with decay rate constant k_{D_1} *or* k_{D_2} which is equal to that determined from the single-exponential rise (with rate constant k_R) or decay (with rate constant k_{D_2}) curve of band B_1, respectively. For ^{3}MAQ* in ethanol or EPA at room temperature (or in EPA at 77 K), we thus conclude that intermolecular hydrogen-atom abstraction by the carbonyl oxygen from ethanol is extremely slow compared with intramolecular hydrogen-atom transfer from the methyl group to the carbonyl oxygen. This is supported by the facts that the quantum yield (0.009)[25] for formation of $MAQH_2$ from MAQ in ethanol at room temperature is very small and elevation of the sample temperature up to room temperature (after photolysis of MAQ in EPA at 77 K) reflects no formation of $MAQH_2$ (and thus negligibly small generation of MAQH$^\bullet$) at 77 K.

Intermolecular Hydrogen-Atom Abstraction of the Carbonyl Oxygen from Ethanol in the Third Excited Singlet or Triplet State of DMAQ. Undoubtedly, the absorption spectral change shown in Figure 11b indicates formation of 1,4-dimethyl-9,10-dihydroxyanthracene ($DMAQH_2$) from DMAQ. Interestingly, however, formation of $DMAQH_2$ is observed only upon 313 nm steady-state photolysis of DMAQ in ethanol or EPA at room temperature. As stated previously, no formation of $DMAQH_2$ upon 366 nm steady-state photolysis of DMAQ cannot be ascribed to formation of $DMAQH_2$ followed by its subsequent photochemical conversion to the original anthraquinone (DMAQ). In Figure 11b, a comparison of the dashed arrows with the dashed line (the absorption spectrum of DMAQ recorded at longer wavelengths than 366 nm) indicates that 366 nm excitation should populate not the lowest excited singlet state (^{1}DMAQ*) but the second excited singlet state (^{1}DMAQ**) and that 313 nm excitation may populate not only ^{1}DMAQ** but also the third excited singlet state (^{1}DMAQ***). We thus suppose that only the carbonyl oxygen of ^{1}DMAQ*** [or the third excited triplet state (^{3}DMAQ***)] abstracts a hydrogen atom from ethanol generating the semiquinone radical (DMAQH$^\bullet$) followed by formation of $DMAQH_2$. Probably, this intermolecular hydrogen-atom abstraction my require an activation energy resulting in no generation of DMAQH$^\bullet$ (and then no formation of $DMAQH_2$) at 77 K. Since 313 nm steady-state photolysis of DMAQ in EPA at 77 K gives rise to formation of MT_b, temperature- dependent ^{1}DMAQ*** (or ^{3}DMAQ***) $\rightarrow$ DMAQH$^\bullet$ intermolecular hydrogen-atom abstraction from ethanol may compete with temperature-independent ^{1}DMAQ*** $\rightarrow$ ^{1}DMAQ** $\rightarrow$ ^{1}DMAQ* cascade internal conversion. Using the 266 and 308 nm excitation light pulses from a Nd^{3+}:YAG laser (fwhm = 5 ns) and an excimer laser (fwhm = 6 ns), respectively, nanosecond laser photolysis of DMAQ in ethanol at room temperature is performed but the results (the transient absorption spectra and the intensity changes of transient absorptions with time) obtained are found to be identical to those obtained by 347.2 nm excitation. Hence, no clear observation of an absorption band responsible for DMAQH$^\bullet$ can be ascribed to its negligibly small yields. In fact, 313 nm steady-state photolysis of DMAQ in ethanol at room temperature reveals an extremely small quantum yield for formation of $DMAQH_2$ even compared with that (0.009) for formation of $MAQH_2$ from MAQ.

Conclusion

For planar alkylanthraquinones (MAQ and DMAQ), we have shown that both the lowest excited singlet and triplet states undergo intramolecular hydrogen-atom transfer (from the methyl group to the carbonyl oxygen) generating the corresponding excited biradicals followed by formation of the methides. This hydrogen-atom transfer is essentially identical to that observed for highly strained 1,4-hexyl-bridged anthraquinone except that the ground-state singlet biradical and its methide formed from the latter compound can exist as two individual species owing to the lack of coplanarity of the π-moiety.[7] Interestingly, not the lowest excited triplet state but the third excited singlet or triplet state of DMAQ may abstract a hydrogen atom from ethanol, generating DMAQH$^\bullet$ followed by formation of $DMAQH_2$. In contrast, formation of $MAQH_2$ from MAQ can be observed irrespective of the excitation wavelength, indicating that the lowest excited triplet state of MAQ also abstracts a hydrogen atom from ethanol. This can be ascribed to the existence of one carbonyl group not adjacent to the methyl group. In this sense, the photochemical behavior of the lowest excited triplet state of MAQ is dual; i.e., one reaction (major) is identical with that of DMAQ and the other reaction (very much minor) is identical with that of anthraquinone.

Acknowledgment. This work was supported by a Grant-in-Aid for Priority-Area-Research on Photoreaction Dynamics from the Ministry of Education, Science, Sports and Culture of Japan (No. 06239101).

References and Notes

(1) Hamanoue, K.; Nakayama, T.; Kajiwara, Y.; Yamaguchi, T.; Teranishi, H. *J. Chem. Phys.* **1987**, *86*, 6654. Hamanoue, K.; Nakayama, T.; Tsujimoto, I.; Miki, S.; Ushida, K. *J. Phys. Chem.* **1995**, *99*, 5802.

(2) Nakayama, T.; Yamaguchi, T.; Ushida, K.; Hamanoue, K.; Miki, S.; Matsuo, K.; Yoshida, Z. *Chem. Phys. Lett.* **1988**, *148*, 259.

(3) Hamanoue, K.; Sawada, K.; Yokoyama, K.; Nakayama, T.; Hirase, S.; Teranishi, H. *J. Photochem.* **1986**, *33*, 99. Hamanoue, K.; Nakayama, T.; Sawada, K.; Yamamoto, Y.; Hirase, S.; Teranishi, H. *Bull. Chem. Soc. Jpn.* **1986**, *59*, 2735. Hamanoue, K.; Nakayama, T. *Res. Chem. Intermed.* **1996**, *22*, 189.

(4) Miki, S.; Matsuo, K.; Yoshida, M.; Yoshida, Z. *Tetrahedron Lett.* **1988**, *29*, 2211.

(5) Nakayama, T.; Amijima, Y.; Ushida, K.; Hamanoue, K. *Chem. Phys. Lett.* **1996**, *258*, 663.

(6) Nakayama, T.; Nagahara, T.; Miki, S.; Hamanoue, K. *Chem. Phys. Lett.* **1997**, *266*, 601. Nakayama, T.; Nagahara, T.; Miki, S.; Hamanoue, K. *Chem. Lett.* **1997**, 597.

(7) Nakayama, T.; Hamana, T.; Miki, S.; Hamanoue, K. *J. Chem. Soc., Faraday Trans.* **1996**, *92*, 1473.

(8) Nakayama, T.; Honma, C.; Miki, S.; Hamanoue, K. *Chem. Phys. Lett.* **1993**, *213*, 581. Hamana, T.; Miki, S.; Hamanoue, K. *Chem. Lett.* **1996**, 87.

(9) Fieser, L. F. *Organic Experiments*; Maruzen: Tokyo, 1964; p 196.

(10) Nakayama, T.; Amijima, Y.; Ibuki, K.; Hamanoue, K. *Rev. Sci. Instrum.* **1997**, *68*, 4364.

(11) Ushida, K.; Nakayama, T.; Nakazawa, T.; Hamanoue, K.; Nagamura, T.; Mugishima, A.; Sakimukai, S. *Rev. Sci. Instrum.* **1989**, *60*, 617.

(12) The rate constants with experimental errors are as follows: $k'_R = k'_{D_1} = (5.7 \pm 0.1) \times 10^6\ s^{-1}$, $k'_{D_3} = (4.9 \pm 0.2) \times 10^4\ s^{-1}$, and $k'_{D_4} = (4.2 \pm 0.2) \times 10^3\ s^{-1}$ for MAQ, and $k'_R = k'_{D_1} = (9.4 \pm 0.1) \times 10^6\ s^{-1}$, $k'_{D_3} = (1.8 \pm 0.2) \times 10^4\ s^{-1}$, and $k'_{D_4} = (2.3 \pm 0.2) \times 10^3\ s^{-1}$ for DMAQ.

(13) The rate constants with experimental errors are as follows: $k_R = k_{D_1} = (1.5 \pm 0.3) \times 10^7\ s^{-1}$, $k_{D_3} = (5.2 \pm 0.2) \times 10^5\ s^{-1}$, $k_{D_4} = (1.5 \pm 0.2) \times 10^5\ s^{-1}$, and $k_{D_2} = (5.1 \pm 0.2) \times 10^4\ s^{-1}$ for MAQ, and $k_R = k_{D_1} = (1.8 \pm 0.2) \times 10^7\ s^{-1}$, $k_{D_3} = (7.4 \pm 0.2) \times 10^5\ s^{-1}$, $k_{D_4} = (1.2 \pm 0.3) \times 10^5\ s^{-1}$, and $k_{D_2} = (2.7 \pm 0.3) \times 10^4\ s^{-1}$ for DMAQ.

(14) Gritsan, N. P.; Shvartsberg, E. M.; Russkikh, V. V.; Khmelinski, I. V. *Russ. J. Phys. Chem.* **1990**, *64*, 1660 (translated from *Zh. Fiz. Khim.* **1990**, *64*, 3081).

(15) Gritsan, N. P.; Khmelinski, I. V.; Usov, O. M. *J. Am. Chem. Soc.* **1991**, *113*, 9615.

(16) Haag, R.; Wirz, J.; Wagner, P. J. *Helv. Chim. Acta* **1977**, *60*, 2595.

(17) Scaiano, J. C. *Chem. Phys. Lett.* **1980**, *73*, 319.

(18) Al-Soufi, W.; Eychmüller, A.; Grellmann, K. H. *J. Phys. Chem.* **1991**, *95*, 2022.

(19) Grellmann, K. H.; Weller, H.; Tauer, E. *Chem. Phys. Lett.* **1983**, *95*, 195.

(20) Baron, U.; Bartelt, G.; Eychmüller, A.; Grellmann, K. H.; Schmitt, U.; Tauer, E.; Weller, H. *J. Photochem.* **1985**, *28*, 187.

(21) Hamanoue, K.; Yokoyama, K.; Kajiwara, Y.; Nakajima, K.; Nakayama, T.; Teranishi, H. *Chem. Phys. Lett.* **1984**, *110*, 25. Hamanoue, K.; Nakayama, T.; Tanaka, A.; Kajiwara, Y.; Teranishi, H. *J. Photochem.* **1986**, *34*, 73.

(22) Porter, G.; Tchir, M. F. *J. Chem. Soc. A.* **1971**, 3772.

(23) Wagner, P. J.; Giri, B. P.; Scaiano, J. C.; Ward, D. L.; Gube, E.; Lee, F. L. *J. Am. Chem. Soc.* **1985**, *107*, 5483.

(24) Nakayama, T.; Hamanoue, K.; Hidaka, T.; Okamoto, M.; Teranishi, H. *J. Photochem.* **1984**, *24*, 71. Nakayama, T.; Torii, Y.; Nagahara, T.; Hamanoue, K. *J. Photochem. Photobiol. A: Chem.* **1998**, *119*, 1.

(25) The quantum yield (0.009) is determined by comparison of the intensity decrease in the absorption spectrum upon photolysis of MAQ with that of anthraquinone, because the quantum yield for photoreduction of anthraquinone in ethanol at room temperature is unity.[26]

(26) Hamanoue, K.; Nakayama, T.; Yamamoto, Y.; Sawada, K.; Yuhara, Y.; Teranishi, H. *Bull. Chem. Soc. Jpn.* **1988**, *61*, 1121. Hamanoue, K.; Nakayama, T.; Sasaki, H.; Ikenaga, K; Ibuki, K. *Bull. Chem. Soc. Jpn.* **1992**, *65*, 3141.